JPhys Materials

PAPER • OPEN ACCESS

Interaction of xanthan gums with galacto- and glucomannans. part I: molecular interactions and synergism in cold gelled systems

To cite this article: Christine Schreiber *et al* 2020 *J. Phys. Mater.* **3** 034013

IOP Publishing J. Phys. Mater. 3 (2020) 034013 https://doi.org/10.1088/2515-7639/ab9ac8

Journal of Physics: Materials

OPEN ACCESS

RECEIVED
21 April 2020

REVISED
26 May 2020

ACCEPTED FOR PUBLICATION
9 June 2020

PUBLISHED
7 July 2020

PAPER

Interaction of xanthan gums with galacto- and glucomannans. part I: molecular interactions and synergism in cold gelled systems

Christine Schreiber[1], **Marta Ghebremedhin**[1], **Birgitta Zielbauer**[1], **Natalie Dietz**[2] **and Thomas A Vilgis**[1]

[1] Max-Planck-Institute for Polymer Research, Department of Polymer Theory, Food Science and Statistical Physics of Soft Matter, Ackermannweg 10, 55128 Mainz, Germany

[2] Jungbunzlauer Ladenburg GmbH, Jungbunzlauer Suisse AG, Dr Albert-Reimann-Straße 18, 68526 Ladenburg, Germany

E-mail: schreiber@mpip-mainz.mpg.de **and** vilgis@mpip-mainz.mpg.de

Keywords: xanthan gum, guar gum, locust bean gum, konjac glucomannan, cold gelled systems, molecular interactions, synergism

Abstract

Several studies have investigated xanthan-guar gum (XG-GG), xanthan-locust bean gum (XG-LBG), and xanthan-konjac glucomannan (XG-KGM) blends but little attention has been paid to the physical interactions between the hydrocolloids on a molecular basis. This requires a consistent sample preparation. Often, LBG is heated up to dissolve completely and then xanthan is added, whereas mixtures with guar gum are prepared at room temperature. To understand the synergy during gelation it is necessary to investigate the xanthan-hydrocolloid solutions in the non-heated state because it sets and controls the preferred initial conditions for the given interactions by chain stiffness, charge and polarity under different concentrations

In this first part of the publication we focused on blends which are all prepared at room temperature and analysed the molecular interaction in these cold mixed systems. Regarding this, we used Rheology and AFM measurements to characterise the single molecules and the mixing behavior and synergism of the blends. We found, that the cold mixed systems are not stable at room temperature and show a phase separation after one and two days, according to the sample, but are stable when stored at 4 °C. Further, these mixing and demixing properties are highly corresponding to the synergism. Blends with xanthan-guar gum with the weakest mixing properties show the weakest synergism, whereas xanthan-konjac blends with a good mixing behavior exhibit the highest synergism. From the AFM micrographs it was observed that XG-KGM gave most homogeneous mixtures, whereas XG-LBG and XG-GG showed strong phase separation. Based on our experimental results and the characteristics of the molecules such as molecular size, shape and side chains we propose molecular models to explain the physical interactions in these systems which are supported by atomic force microscopy.

1. Introduction

Xanthan gum (XG), guar gum (GG), locust bean gum (LBG) and konjac glucomannan (KGM) are common ingredients used to optimise the viscoelastic properties of food, body and care products. They are used in body and dental care products, pharmaceutical products and in food industry for e.g. sauces, dressings, bakery products, beverages, desserts and ice cream to adjust the viscosity of the product [1]. The understanding of molecular interactions requires multiscale details of the polymers, i.e. their local molecular structure on monomer scales and their behavior of mesoscales.

Xanthan gum is a strongly negatively charged polymer with a high molecular weight and is produced by the microorganism *Xanthomonas campestris* in a fermentation process. It can be hydrated in cold water and forms viscous liquids with a pseudoplastic flow behaviour [2]. It has a rigid structure which helps to retain the viscosity even under heating and is stable over a wide pH range and tolerant of high salt concentrations. [3, 4]

The galactomannans guar gum and locust bean gum and the glucomannan konjac are extracted from plants, meaning from the seeds of the guar plant, the seeds of the locust-tree and from the tuber of the devil's tongue. They are neutral but polar polysaccharides with a high molecular weight. Like Xanthan they are hydratable in water, but LBG needs to be heated to be completely soluble. [5, 6]

Xanthan gum shows macroscopically synergistic effects with GG, LBG and KGM when mixed together, i.e. the combination of the two components exhibits a higher increase of the viscosity as expected for the addition of the properties of the single components. Cohesive, thermoreversible gels are formed with LBG and KGM, the blend with GG exhibits thickening effects. [7–9]

Like cellulose, xanthan gum consists of a backbone of β-(1→4)-D-glucose units. Every second glucose molecule has a side chain of two mannose residues with a glucuronic acid residue between them. The mannose residue closer to the backbone has an acetyl group at its C-6 position, the more distant mannose residue has a pyruvate group between its C-4 and C-6 atom [10, 11]. The content of acetate and pyruvate groups varies according to fermentation conditions. They are typically at 30%–40% for pyruvate groups and between 60%–70% for acetyl groups [12], but the groups also can be removed [13, 14].

The galactomannans locust bean gum and guar gum are composed of a linear chain of (1→4) linked β-D-mannopyranosyl units with (1→6)-α-D-galactopyranosyl residues as side chains. The ratios of mannose to galactose and the distribution of the side chains are different. Guar gum has a ratio of 2:1 mannose:galactose and a random distribution of the side chains [15–17]. LBG has a ratio of 4:1 but here the galactose residues occur in blocks, meaning that LBS has 'smooth' and 'hairy' regions [18, 19].

Cairns *et al* found that it is necessary to heat the mixture above the helix-coil transition temperature of xanthan and let it cool down to form gels. [20, 21] The present studies confirm this observation and we will discuss our results of the heated gels in the second part of the publication. The aim of this work is to characterise the molecular interactions of different xanthan gums in a mixture with guar gum, locust bean gum and konjac glucomannan in non-heated systems. Special focus is set on the fact that these systems are all prepared at room temperature and that the mixed systems do not undergo any further heating as it is the case in many other publications. At higher temperature a conformational change of xanthan gum and konjac glucomannan is assumed, which alters the gelation process significantly.

In this part of the publication we investigated the behaviour of the 'cold gelled systems' and analysed the molecular interactions in these non-heated systems. We propose a model of the interactions between xanthan and mannan based on our results. For our investigation we characterised the single components and the mixed systems by rheology and atomic force microscopy. Different types of xanthan gum were used to study the influence of the molecular structure on the interactions. In different other studies rheology was also used to characterise the interaction between xanthan and mannans, e.g. by determining the viscosity, the dynamic modulus, and storage modulus [7, 9, 22–25]. In this study we performed amplitude sweeps and focused on the storage (G') and loss moduli (G") of the systems. With these parameter we get insight in the inner structure of the hydrogels and can provide conclusions about breaking behavior and network structures of the hydrogels. Teckentrupp & Al-Hammood *et al* and Moffat *et al* used AFM to study the conformation and secondary structure of xanthan molecules. They show that xanthan exhibits a double-stranded helical form but also a single-stranded disordered form depending on the chemical composition of the xanthan gum. [26, 27] Based on their methods we prepared our samples for the single components and the xanthan-mannan mixtures for the AFM measurements.

In the second part of the paper, the heated systems are in the focus of interest. We characterised the gelling process of the different mixtures and the influence of salt to the gelation. Also here, we propose a model of the interactions between the molecules explaining the gelation.

2. Materials and methods

2.1. Samples and preparation

The xanthan samples were obtained from Jungbunzlauer Ladenburg GmbH in Germany. Xanthan gum 1 (XG1) possessed no further modification, xanthan gum 2 (XG2) contained less pyruvate-groups than the unmodified xanthan and was shorter than the two other xanthans, and xanthan gum 3 (XG3) contained marginally less acetyl-groups. Locust bean gum (VIDOGUM L 175), guar gum (VIDOGUM G200 I), and konjac glucomannan (VIDOGUM KJ-II) were received from UNIPEKTIN AG, Eschenz, Switzerland.

The hydrocolloids were dissolved in a concentration of 0.5% w w^{-1} while considering the moisture content of the sample. The moisture content was determined by a halogen moisture analyser (Mettler-Toledo HR83) in a triple determination and the amount of sample was calculated by the following equation for a total volume of 10 g:

$$m_x = \frac{0.5\,\% * 10\,g}{100\,\% - MC\%}$$

(m_x—mass of xanthan, MC—moisture content).

The samples were weighed with a precision of ± 0.0002 g to reduce variations in rheology measurements. The samples were dissolved in Milli-Q water to avoid any salt effects and stirred overnight (XG 350 rpm, mannans 500 rpm) at room temperature to dissolve completely. Since locust bean gum is partly insoluble in cold water, the sample was heated up to 90 °C–95 °C for 10 min and then stirred overnight. Locust bean gum, guar gum and konjac glucomannan were centrifuged at 10 350 rpm (15 090 g) for 20 min to remove cell residues.

The mixed solutions were prepared in different ratios with the solved samples as described above and stirred for 5 min at 1200 rpm without any additional heating at room temperature. The blends were incubated for 30 min to ensure a full formation of the hydrogel.

2.2. Rheology

To analyse and compare the synergistic effect of the mixtures of XG with GG, LGB and KGM amplitude sweeps of the blends at different ratios were conducted. The samples are expected to show a linear region of storage and loss modulus followed by a decrease when the inner structure breaks. In addition, the samples should exhibit different values for the moduli according to the system and synergistic interactions. A Discovery HR-3 Rheometer of TA instruments was used for the measurements. The blends were measured with a cone-plate geometry of 40 mm in diameter, a cone angle of 2° and a shearing gap of 56 μm from tip of the cone to the plate. To determine the storage modulus *G*' and loss modulus *G*" of the samples an amplitude sweep was measured in a triple determination for each blend and ratio. In order not to disturb the hydrogel structure the samples were placed on the geometry with a spoon and any overflowing sample material was carefully removed with a spatula. The measurements were done at 25 °C with a soak time of 120 s, frequency of $f = 1$ Hz, shear strain of $\gamma = 0.02$–10 000%, and 10 points per decade in a logarithmic sweep. The limit of the LVE region was determined with a tolerance range of deviation for G' of 5%.

2.3. AFM

AFM measurements were performed to visualise the size and conformation of the individual molecules and to gain insight into the distribution of the different molecules in the mixtures.

The samples for AFM measurements were diluted to a concentration of 10 μg ml^{-1}, pipetted onto a freshly cleaved mica plate, incubated for 30 s to allow the molecules to adhere on the surface and then dried under a gentle flow of argon to ensure that the surface of the droplet is not affected [26]. The topographical imaging was done using a Torsion TUNA 2 Multimode V by Bruker with an EVLR scanner in tapping mode. The cantilevers OTESPA, with a resonance frequency of $f = 300$ kHz, a spring constant of 42 N m^{-1} and aluminium coating, were also received from Bruker. The images were scanned with a resolution of 512 × 512 pixels and the scan rate was varied between 0.5 and 0.8 Hz according to the sample. The apparent persistence length of XG and the contour length of the mannans were determined using ImageJ. Some of the selected sections or molecules are marked and shown in the images in part 2.1.

3. Results and discussion

3.1. AFM pictures of the single components

Figure 1 shows AFM pictures of the different xanthan types. Due to the sample preparation the molecules are projected from a 3D dimension into a 2D surface. This may cause some exaggerated stretching of the molecule during the adhesion on the mica surface but the general features of the molecule are maintained and allow a comparison of the rigidity and flexibility of the molecules. The polymer chains seem to have rigid areas but also exhibit a certain flexibility which can be seen in the curved structures. As the molecules are forced into a 2D conformation and are not in their natural state an apparent persistence length was determined for a relative comparison of the stiffness of the molecules. The measured lengths are listed in table 1. The rigidity of the structures was determined by calculating the minimal apparent persistence length. This value represents the earliest possibility for the polymer chain to change its orientation. As can be seen in table 1 the most rigid structure was found in the samples made with XG2 with less pyruvate groups. This observation also confirms the previous results on mechanical properties of the three xanthan types; XG1 and XG3 exhibiting a semi-flexible and XG2 showing a rigid structure [28].

Figure 2 exhibits the corresponding AFM images of the samples prepared with the aforementioned galacto- and glucomannans. Table 2 lists the calculated contour lengths. However, due to the small number of measured molecules these numbers offer a rather rough comparison of the structural dimensions. Guar gum is a comparatively long and flexible molecule, whereas locust bean gum and konjac glucomannan are considerably shorter and more rigid.

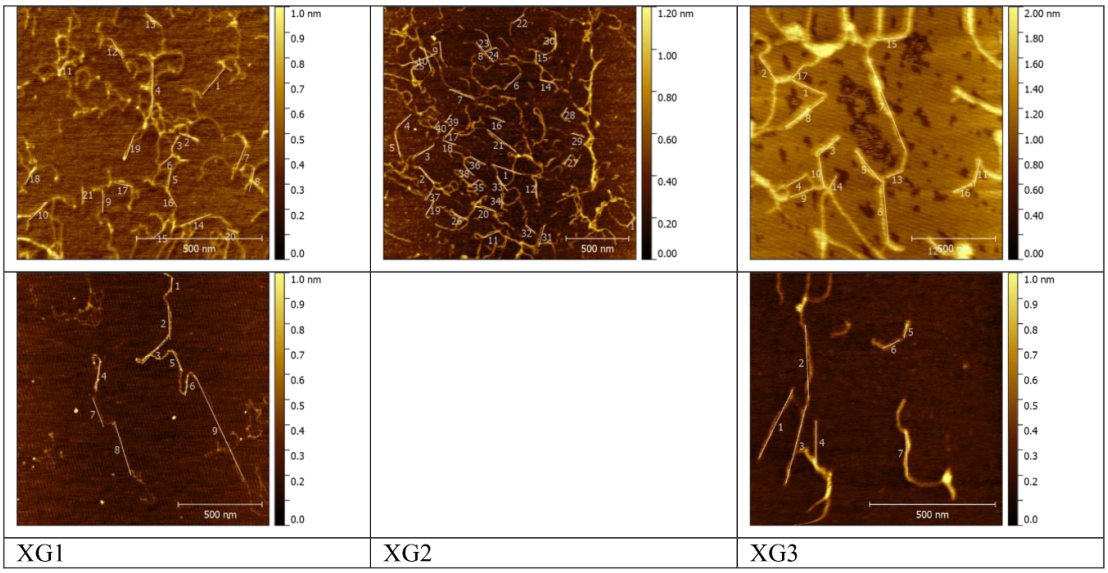

Figure 1. AFM pictures of the different xanthan types. All of them have stiff and flexible domains as indicated directly in the pictures by scale lines.

Table 1. Apparent persistence length of XG1, XG2 and XG3.

	XG1	XG2	XG3
Average (nm)	130	138	163
Standard deviation (nm)	121	52	108
Minimum (nm)	42	61	37
Maximum (nm)	678	258	607

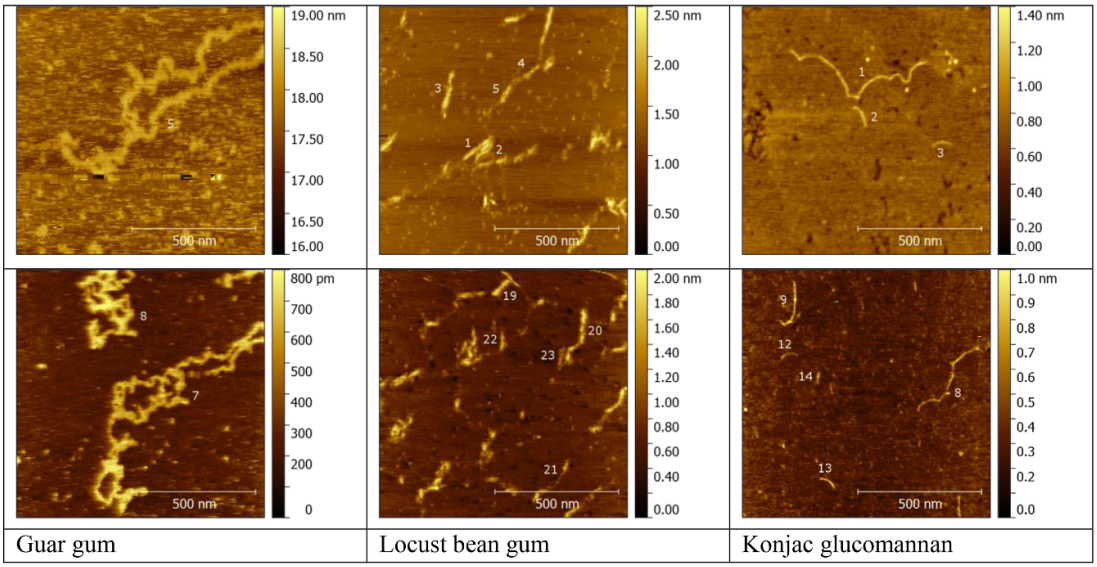

Figure 2. AFM pictures of guar gum, locust bean gum and konjac glucomannan. Guar gum is a very flexible and long molecule, whereas locust bean gum and konjac glucomannan are shorter and more rigid.

3.2. Mixing and demixing behaviour of xanthan-mannan blends

During the sample preparation it was observed that the blends are not thermodynamically stable at room temperature and separate after a certain time.

Figure 3 shows blends of xanthan with LBG, GG and KGM as freshly prepared samples and after a period of one and two days. The samples were stained with toluidine blue for a better visibility. The separation of

Table 2. Contour length of guar gum, locust bean gum and konjac glucomannan.

	Guar gum	Locust bean gum	Konjac glucomannan
Average (nm)	1670	98	189
Standard deviation (nm)	1312	55	188
Minimum (nm)	516	35	43
Maximum (nm)	3532	238	770

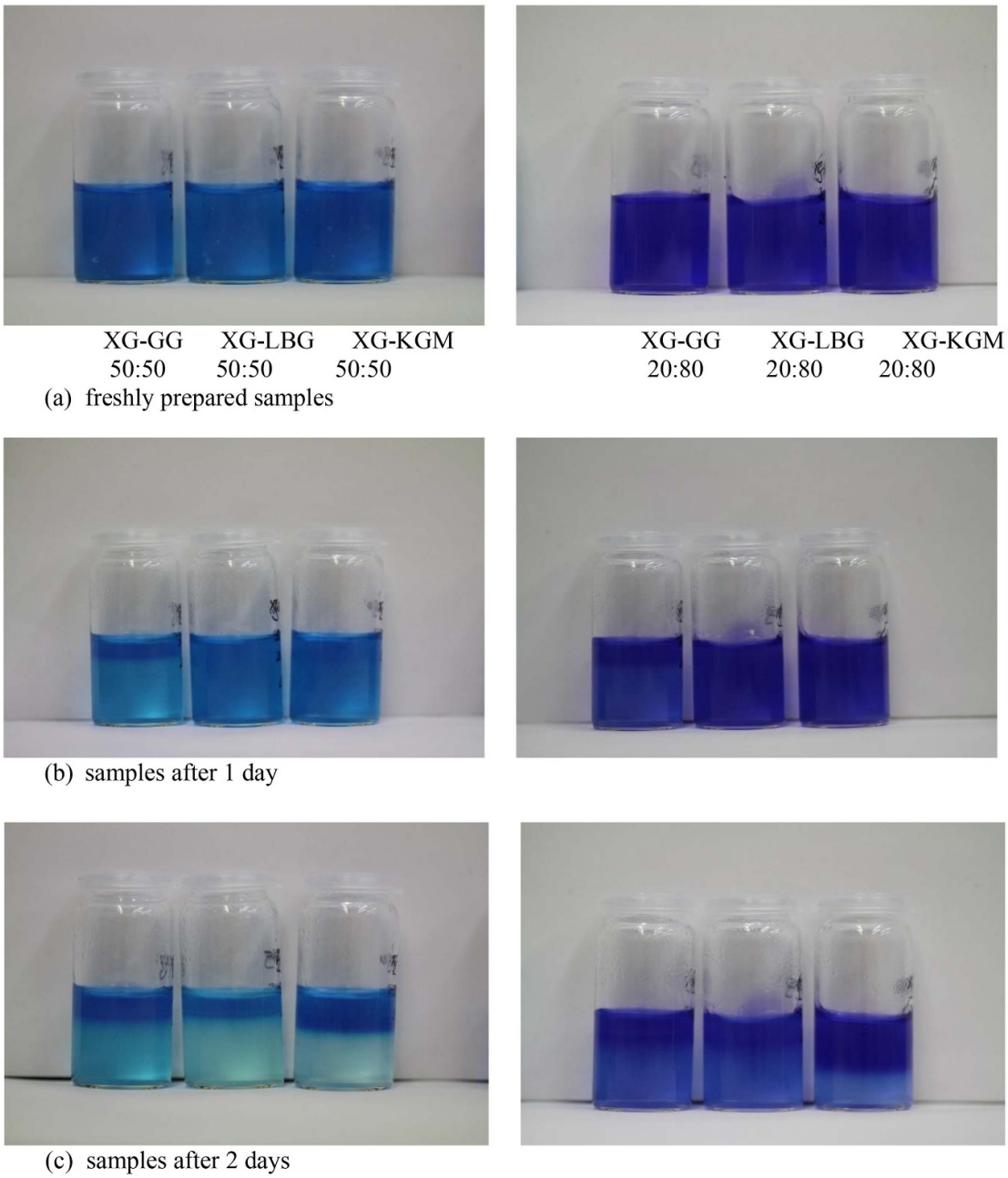

Figure 3. Blends of xanthan with LBG, GG and KGM, stained with toluidine blue for a better visibility.

xanthan-guar gum (XG-GG) is visible to the naked eye after 1 d, xanthan-locust bean gum (XG-LBG) and xanthan-konjac glucomannan (XG-KGM) after 2 d.

The picture in figure 4 shows xanthan-guar blend in different ratios, demonstrating that the demixing is independent from the ratio of the blends and the pure KGM sample stained with toluidine blue does not separate like the mixtures. Therefore, the separation of the blends is not based on floating of the dye. The phases of the blends had different textures after several days. The picture on the right side in figure 5 demonstrates the changed properties/textures of XG-KGM after 17 d.

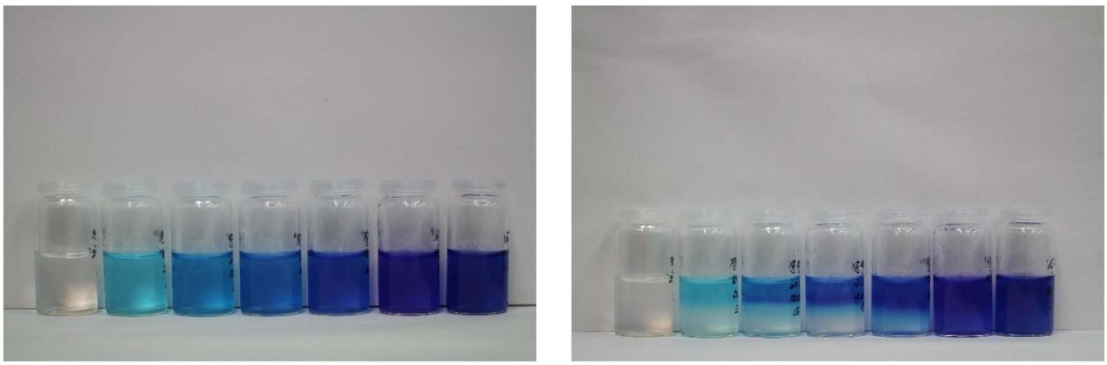

Figure 4. Phase separation of XG-KGM in various ratios. The samples were stained with toluidine blue for better visibility.

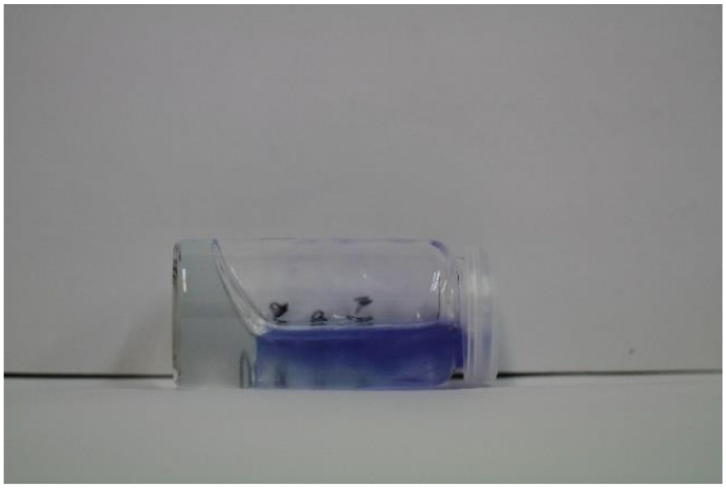

Figure 5. Separation and different textures of the phases of XG-KGM. The transparent phase has viscoelastic, the stained phase liquid properties. The sample was stained with toluidine blue for better visibility.

Samples stored at 4 °C did not separate even after some weeks. This means that although at room temperature the blends are not at a thermodynamic equilibrium, the Brownian motion of the molecules is heavily constrained at lower temperatures, thus leading to a more stable blend.

Figure 6(a) shows the storage and loss moduli of XG1-GG in a ratio of 50:50 after specified times at room temperature. The blend is stable for 10 h at room temperature, as can be seen in the graph. After 20 h there is a significant decrease of the storage modulus. The blend of XG2-GG is also stable for a period of 10 h at room temperature and shows a similar decrease of the storage modulus after 20 h (figure 7(a)). The properties of the blend change and the mixture exhibits a more viscous character. Consequently, all the following measurements were conducted between 30 min to 10 h after sample preparation, thus keeping the measurements in the rheologically stable range.

In order to compare the stability of the blends over a prolonged period of time at different temperatures, freshly prepared samples were refrigerated at 4 °C and measured at stated times. As can be seen in figures 6(b) and 7(b) on the right the storage and loss moduli remain unchanged after this period. This confirms the previous results on blend stability at low temperatures.

3.3. Rheology of xanthan-mannan blends

Figure 8 shows examples for amplitude sweeps for the blends of xanthan 1 with guar gum, locust bean gum and konjac glucomannan at the ratio of the highest synergism. The moduli of XG1-GG show a linear behaviour followed by a decline. XG1-LBG and XG1-KGM exhibit a small hump in the loss modulus. This is an indication for a network structure in these blends. These humps occur when parts of the molecular

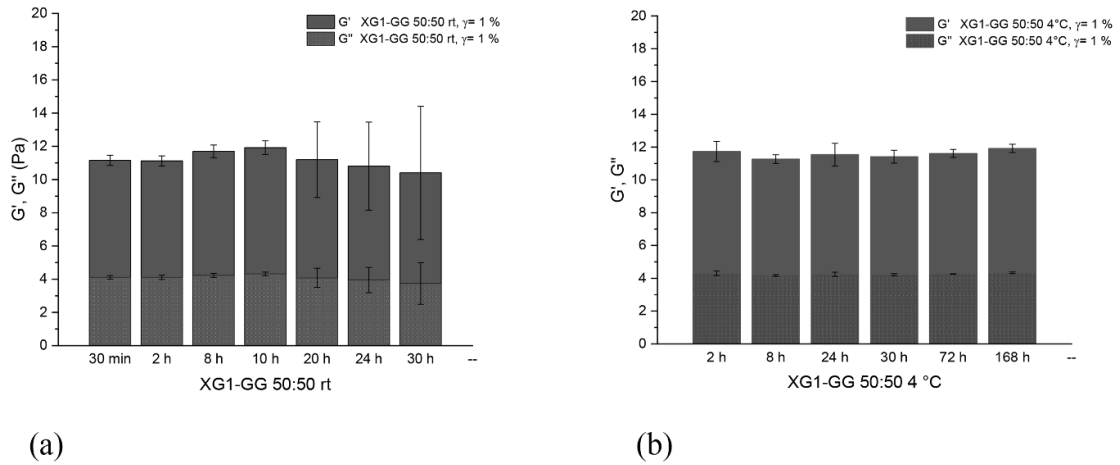

Figure 6. (a) Storage and loss moduli of XG1-GG after different times at room temperature. The storage modulus decreases after a certain time. (b) Storage and loss moduli of XG1-GG after different times stored at 4 °C. The moduli remain constant.

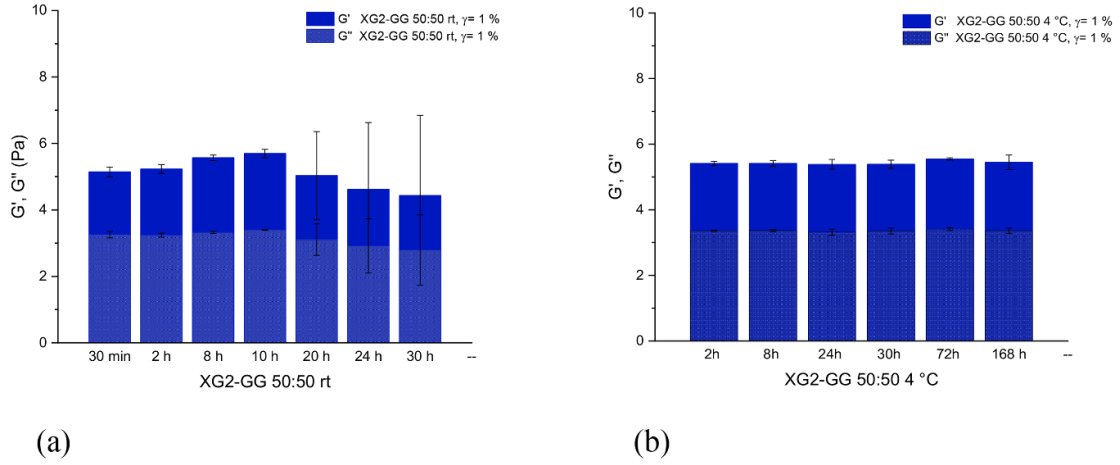

Figure 7. (a) Storage and loss moduli of XG2-GG after different times at room temperature. The storage modulus decreases after a certain time. (b) Storage and loss moduli of XG2-GG after different times stored at 4 °C. The moduli remain constant.

structure defined by the dissolved polymers are destroyed before the internal structure breaks down completely and is typical for gels or high concentrated dispersions with a force network. This happens due to the relative movement of molecules, free chain ends, flexible side chains, long network bridges, or agglomerates which are not substantially embedded in the network [29]. Before the rearrangement of the polymers under high elongations, the entangled and interacting macromolecules need to be cooperatively moved and reorientated, consequently the viscos part increases, before getting lowered again.

Figure 9 displays the storage and loss moduli of the different xanthan blends XG-GG, XG-LBG, and XG-KGM as a function of the xanthan content.

For the xanthan blends with guar gum there is an increase of the storage modulus for all mixing ratios compared to the pure components. The blends of XG3-GG show the highest synergism, followed by XG1-GG and XG2-GG. However, there are no significant differences between the different ratios. For XG2-GG the storage modulus rises to 7 Pa, for XG1-GG up to 12 Pa, and for XG3-GG up to 18 Pa, starting at 2 Pa for pure guar gum. Therefore, the storage modulus of the blend is influenced by that of the xanthan. XG2 with the lowest storage modulus shows the weakest synergism and XG3 with the highest G' shows the largest enhancement. This seems consistent with the fact that XG2 consists of smaller and more rigid molecules than XG1 and XG3, thus leading to less interaction between XG2 and the flexible guar gum [28]. Furthermore, XG3 contains less acetate groups than XG1 and XG2. According to current understanding, the acetate groups stabilise the helix structure of xanthan by hydrogen bridge bonds [12, 30]. Thus, if some of the groups are missing the helix is destabilised, leading to a more flexible xanthan molecule. This in turn improves the interaction with guar gum. Additionally, the XG3 is the largest xanthan with the highest molecular weight,

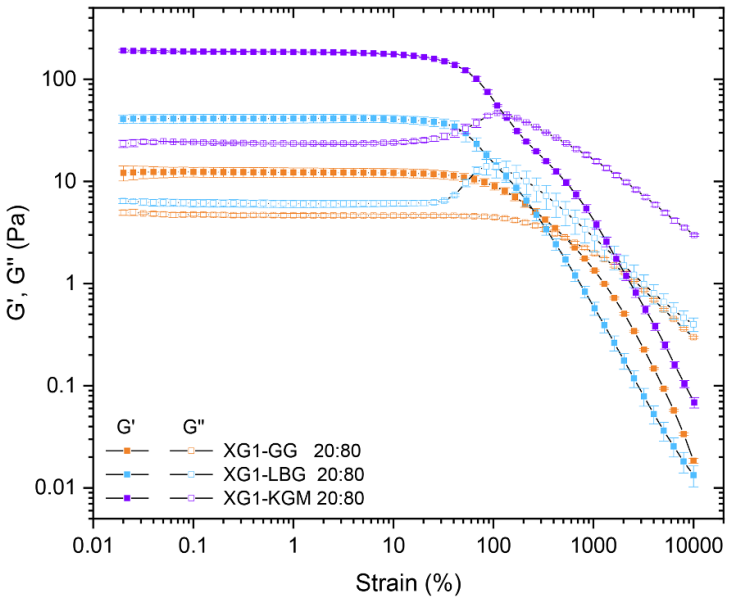

Figure 8. Amplitude-Sweeps of XG1-GG (orange), XG1-LBG (blue), and XG1-KGM (purple) to show the inner structure of the samples.

which allows more entanglements with the guar molecules. Compared to the other mannan systems, the blends with guar gum have the weakest synergism.

The blends with LBG show a higher synergism with an increase of the storage modulus. Starting at 0.2 Pa for pure LBG it increases up to 30 Pa for XG1-LGB, 48 Pa for XG3-LBG, and 79 Pa for XG2-LBG. Compared with the XG-GG blends, the mixtures with LBG exhibit a distinct maximum of the synergistic effect at a ratio of 10:90 for XG3-LBG and 20:80 for XG1-LBG and XG2-LBG. This is an indication for better, or more, specific interactions between xanthan and LBG. A possible explanation for this behavior is the fact that the LBG has less side chains than guar gum, leading to less steric hindrance and improved interactions between the backbones of the LBG and xanthan molecules by hydrogen bonds or van der Waals bonds.

The blends of XG-KGM exhibit the highest synergism effect. The storage moduli rise from 5 Pa for pure KGM up to 185 Pa, 212 Pa and 214 Pa for XG1, XG3 and XG2 respectively. As the storage moduli are of equal dimension, it appears that the KGM is the dominating part of the synergism. The blends with KGM also show a specific maximum for the storage moduli at a ratio of 20:80 for XG1-KGM and XG3-KGM, and 40:60 for XG2-KGM. Thus, it could be concluded that there are more specific interactions between xanthan and konjac than between xanthan and guar gum or LBG. This also supports the assumed interactions between the backbones of the xanthan and mannan molecules. Because konjac contains very few side chains, the interactions between the backbones are better than between xanthan and guar gum or LBG, hence showing a bigger synergism.

Figure 10 illustrates the interactions via hydrogen bonds between the xanthan backbone and the backbones of the mannans as described above. In guar gum the side chains are arranged in triplets or pairs with a random distribution and therefore exhibit poor interactions with xanthan. LBG and konjac both show a higher binding capacity with xanthan due to less flexibility and the lower number of the side chains in LBG and the few side chains in konjac.

3.4. AFM experiments of xanthan-mannan blends

Figures 11–13 show the AFM images of selected XG-mannan blends. The necessary dilution of the samples to conduct the AFM measurements reduces the viscosity rigorous because there are much less molecules to interact, but the general type of chemical interaction, such as H-bonds, is not affected. The AFM images are a projection of the 3D structure of the hydrogels into the 2D structure. So the images give a good indication of the molecule distribution within the samples and support the rheology data and our models of interaction. The results of rheology and AFM are not directly comparable with each other as in rheology the 3D structure is examined and AFM depicts a 2D structure of the sample. The results from rheology show the same behaviour of the blends XG-GG, XG-LBG, and XG-KGM within their system. Thus for the AFM measurements the assumption was made that the blends are also comparable within their group to get an overall picture.

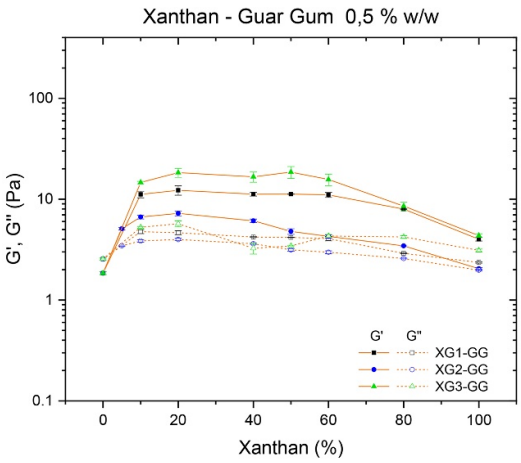

(a) Storage and loss moduli of XG-GG blends depending on the xanthan content

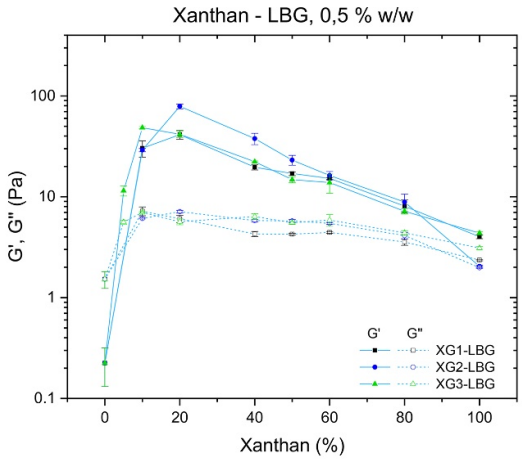

(b) Storage and loss moduli of XG-LBG blends depending on the xanthan content

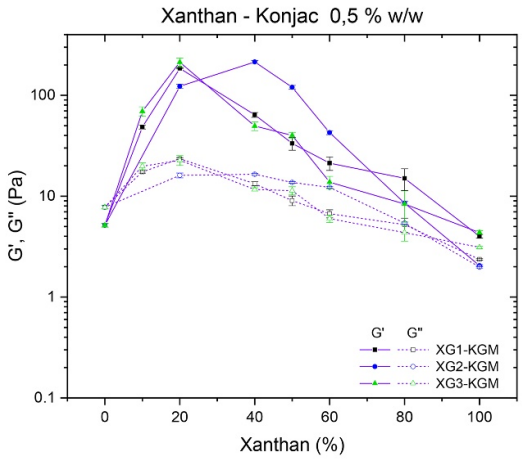

(c) Storage and loss moduli of XG-KGM blends depending on the xanthan content

Figure 9. Storage (G') and loss (G") moduli of (a) XG-GG (orange, (b) XG-LBG (blue), and (c) XG-KGM (purple) as a function of the xanthan content.

The pictures of the xanthan-mannan blends are shown in figure 11. The mixture of xanthan with guar gum exhibits large areas of molecules with a clear-cut structure which can be assigned to xanthan. The large areas with an undefined or 'cloudy' shape can be attributed to mannan. The heterogeneous distribution of these areas reveals the poor miscibility of xanthan and guar gum. The rod-like, rigid structure of xanthan and

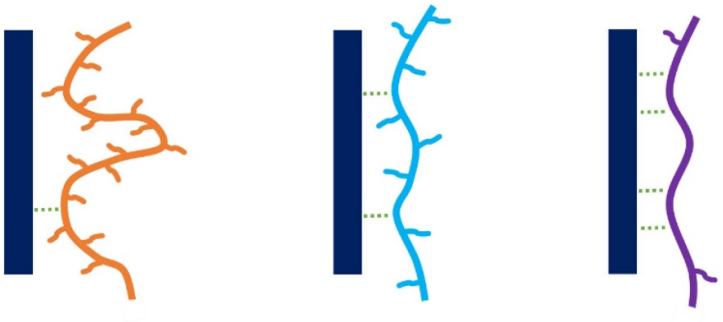

Figure 10. Schematic illustration of the interactions between xanthan and the mannan backbones with the different amount of side chains. From left to right: XG-GG, XG-LBG, and XG-KGM. Xanthan is represented as dark blue rigid rods. GG is shown as a flexible orange line, and LBG and KGM are shown as cyan and violet semi-flexible lines respectively. The size of the molecules is not to scale.

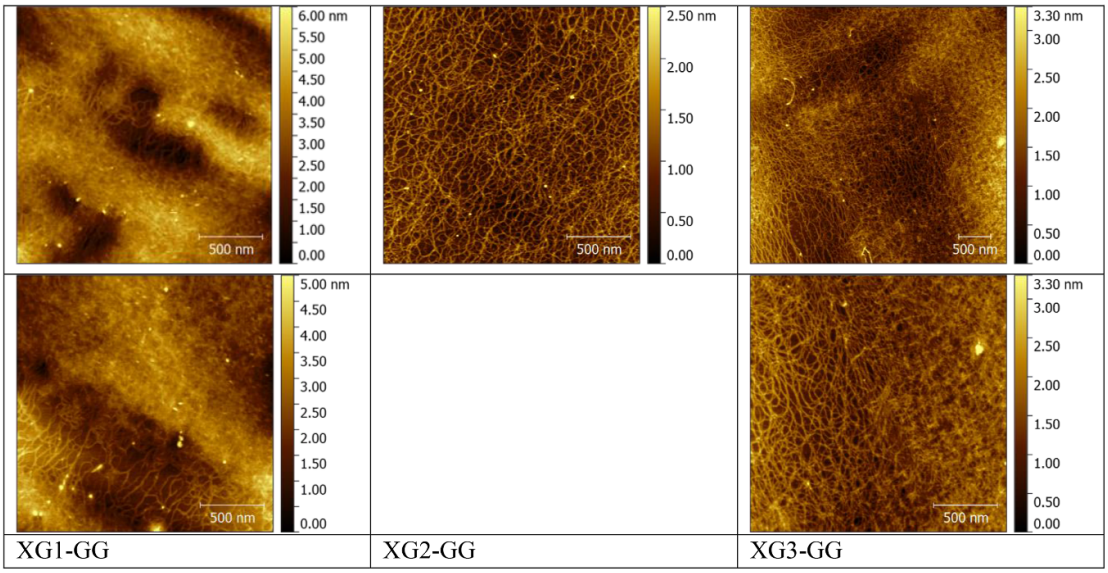

Figure 11. AFM pictures XG-GG (10 μg ml^{-1}).

the flexible guar molecule are not compatible. The entropy driven demixing of the system is expedited by the flexibility and high dynamic of guar gum molecules. The image of XG2-GG shows mainly structures which can be assigned to the xanthan and no obvious areas of guar gum. This seems to be another indication for the heterogeneous distribution of the rigid xanthan and flexible guar molecules.

The blends with locust bean gum show a heterogeneous distribution as well but the different phases are better mixed (figure 12). Several factors contribute to this behavior. The shape of the LBG molecules are more rigid in comparison with guar gum. Xanthan molecules are very constrained in their movement (jamming effect) due to their negative charge. The neutral LBG molecules are not restricted the same way but, however, due to their semi-flexible nature their mobility is slightly reduced. Therefore the entropic demixing is slower than in the XG-GG blends.

The images for XG-KGM display a more homogeneous distribution of the molecules (figure 13). This can also be explained by the similarity of the shapes of the molecules and thereby leading to better miscibility. Similar to the XG-LBG blends the demixing is slower. This could be decelerated furthermore by hydrogen bridge bonds or van der Waals interactions between xanthan and konjac molecules.

Concluding from the AFM pictures, we propose the following model for the molecular distribution of the xanthan and galacto- or glucomannan within their respective mixtures (figure 14). A blend of xanthan and guar gum consists of large, more or less separate phases with only xanthan or guar gum molecules. As the guar gum molecules are neutral and very flexible they do not exhibit a jamming transition like the rod-like, negatively charged xanthan. The high dynamics of the guar molecules promote the entropy-driven demixing of the system and the incompatibility of the molecules in these blends. The short and semi-flexible

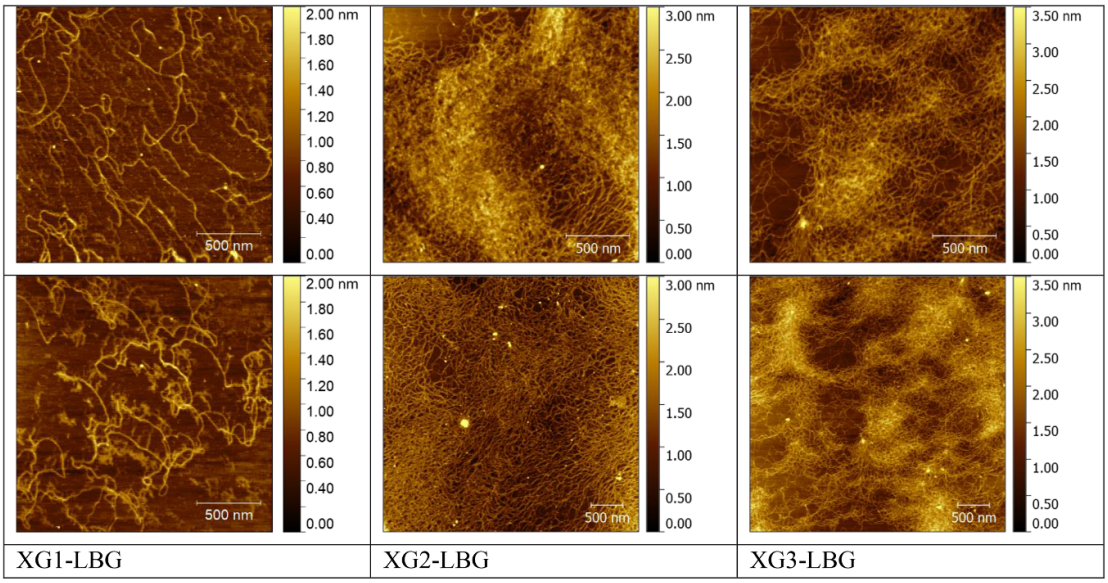

Figure 12. AFM pictures XG-LBG (10 μg ml^{-1}).

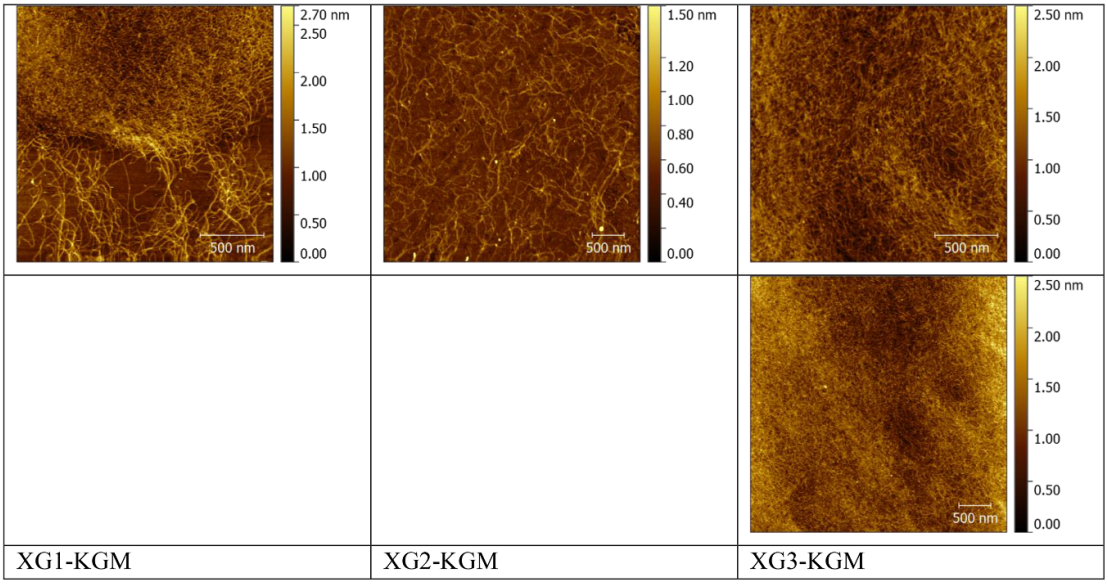

Figure 13. AFM pictures XG-KGM (10 μg ml^{-1}).

LBG molecules allow a better miscibility but areas where one type of molecule dominates strongly also exist. The konjac molecules are also semi-flexible and short, although larger than LBG, and show a full/complete mixing. Due to the more rod-like structure of both the LBG and konjac the mobility of the molecules is limited and the phase separation decelerated.

3.5. LVE range of the mixtures

The behaviour of the LVE ranges also confirms our model proposed above. The mixtures with XG-GG show a long LVE range close to the LVE region of the individual components (figure 15 (a)). This blend consists of large areas of molecules of the same type and thus acts like the individual components in these areas. At the few phase boundaries there are 'heterogeneous' interactions between the molecules via hydrogen bridge bonds. These are easily broken under shear, which in turn reduces the LVE-range.

The mixtures with LBG have a better mixing of the molecules, i.e. less areas with a homogeneous molecular distribution and more phase boundaries, causing a faster disruption of the inner structure under shear.

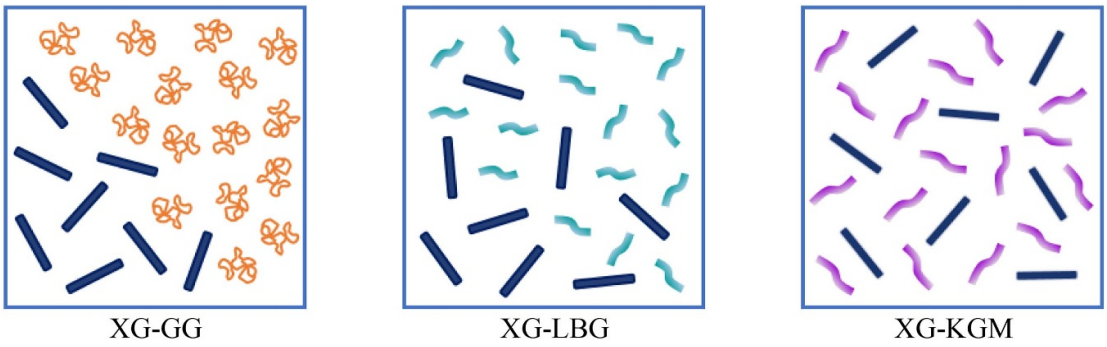

Figure 14. Scheme of the distribution of the molecules in xanthan-mannan blends. Xanthan is represented as dark blue rigid rods, guar gum as orange flexible twine, locust bean gum as cyan semi-flexible rod, as konjac glucomannan as violet semi-flexible rod. The size of the molecules is not true to scale.

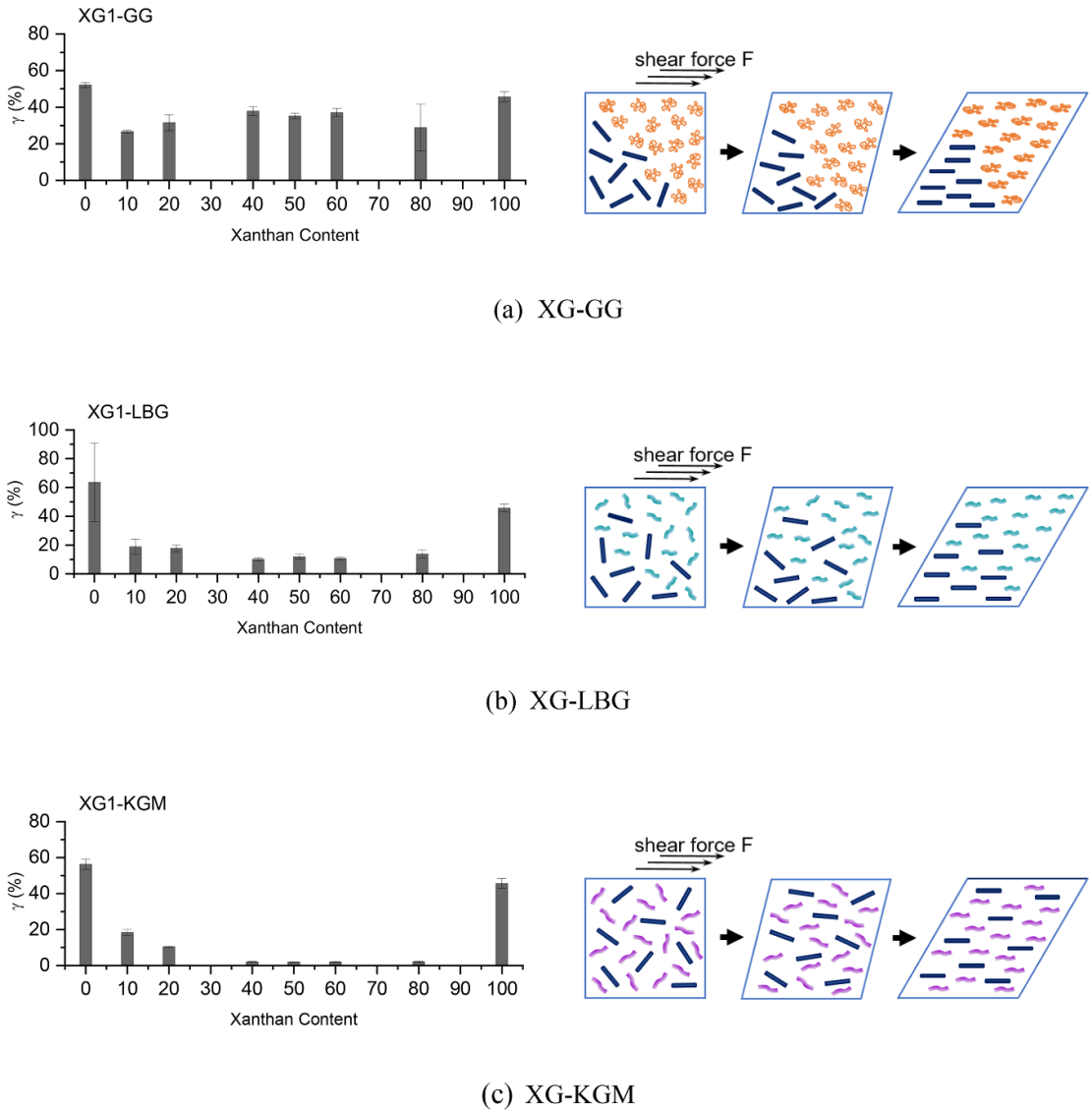

Figure 15. LVE-Range of the mixtures and schematic behaviour under shear. The more phase boundaries and therefore interactions between the different molecules, the shorter the LVE-range.

Finally, the konjac mixtures show a very good mixing behaviour with the shortest LVE-range. Here there are many phase boundaries and hydrogen bonds between the different molecules which can be broken very easily.

4. Conclusion

In this study we investigated xanthan-guar gum, xanthan-locust bean gum, and xanthan-konjac glucomannan blends with a consistent cold sample preparation. The physicochemical properties of the mixtures were analysed with rheology measurements and AFM measurements which give a complete new insight in the molecular distribution of the blends. On the basis of these results we obtained a better understanding of the molecular interactions of the molecules.

The observed phase separation of the xanthan-mannan blends implies that the interactions of the cold mixed hydrocolloids are not permanent. Weak physicals gels are formed with hydrogen bridge bonds and van der Waals interactions between the molecules on the one hand, and an entropy driven tendency to separate on the other.

This effect is the strongest for XG-GG blends. The rod-like xanthan and the large and flexible GG molecules are incompatible and scarcely interact with each other. Therefore, the molecules show a heterogeneous distribution with large areas of the polysaccharides of the same type. Thus, we propose an interaction mechanism between the backbones of the polysaccharides. The numerous side chains of GG further impede these interactions. Thus, XG-GG mixtures show only a weak synergism in increasing the storage modulus of the blend.

The short and semi-flexible LGB molecules can better mix with the rod-like xanthan, leading to a better miscibility and less or smaller areas of molecules of the same type. The amplitude sweeps of XG-LBG indicate a network structure and the enhancement of the storage modulus attains a maximum at a certain ratio. LBG contains less side chains than GG, therefore it is less sterically hindered and can interact better with xanthan via hydrogen bridge and van der Waals bonds.

KGM is also a semi-flexible molecule and shows good mixing properties with xanthan. This and the small number of side chains allow a better interaction and lead to the best synergism effects in the XG-KGM blends. This is also supported by the network structure shown by the rheology, and the better stability at room temperature for XG-KGM blends compared to XG-LBG and XG-GG.

Acknowledgments

The authors acknowledge valuable help and discussions by Dr. Rüdiger Berger for AFM experiments, Dr. Kaloyan Koynov and Andreas Hanewald for assistance and discussions during the rheological measurements (all MPI for Polymer Research).

Furthermore we thank the members of the MPIP soft matter food science group for fruitful discussion and proofreading the manuscript.

Funding

This work was supported by the company Jungbunzlauer (Ladenburg, Germany) by financing Christine Schreibers (labor costs) diploma thesis.

ORCID iDs

Christine Schreiber https://orcid.org/0000-0002-9825-0643
Marta Ghebremedhin https://orcid.org/0000-0001-9225-2587
Thomas A Vilgis https://orcid.org/0000-0003-2101-7410

References

[1] Katzbauer B 1998 Properties and applications of xanthan gum *Polym. Degrad. Stab.* **59** 81–4
[2] Milas M, Rinaudo M, Knipper M and Schuppiser J L 1990 Flow and viscoelastic properties of xanthan gum solutions *Macromolecules* **23** 2506–11
[3] Stephen A M, Phillips G O and Williams P A 2006 *Food Polysaccharides and Their Applications* (Boca Raton, FL: CRC Press)
[4] García-Ochoa F, Santos V E, Casas J A and Gómez E 2000 Xanthan gum: production, recovery, and properties *Biotechnol. Adv.* **18** 549–79
[5] McCleary B, Amado R, Waibel R and Neukom H 1981 Effect of galactose content on the solution and interaction properties of guar and carob galactomannans *Carbohydr. Res.* **92** 269–85
[6] JECFA J F 2008 WHO expert committee on food additives *Compendium of Food Additive Specifications 69th JEFCA Meeting (Rome)* pp 17–24
[7] Tako M and Nakamura S 1985 Synergistic interaction between xanthan and guar gum *Carbohydr. Res.* **138** 207–13
[8] Tako M 1992 Synergistic interaction between xanthan and konjac glucomannan in aqueous media *Biosci. Biotechnol. Biochem.* **56** 1188–92

[9] Abbaszadeh A, Macnaughtan W, Sworn G and Foster T J 2016 New insights into xanthan synergistic interactions with konjac glucomannan: A novel interaction mechanism proposal *Carbohydr. Polym.* **144** 168–77
[10] Jansson P-E, Kenne L and Lindberg B 1975 Structure of the extracellular xanthomonas campestris *Carbohydr. Res.* **45** 275–82
[11] Rinaudo M, Milas M, Lambert F and Vincendon M 1983 1H and 13C NMR investigation of xanthan gum *Macromolecules* **16** 816–9
[12] Tako K and Nakamura S 1989 Evidence for intramolecular associations in xanthan molecules in aqueous media *Agric. Biol. Chem.* **53** 1941–6
[13] Tako M and Nakamura S 1984 Rheological properties of deacetylated xanthan in aqueous media *Agric. Biol. Chem.* **48** 2987–93
[14] Tako M and Nakamura S 1988 Rheological properties of depyruvated xanthan in aqueous media *Agric. Biol. Chem.* **52** 1585–6
[15] Heyne E and Whistler R L 2005 Chemical composition and properties of guar polysaccharides *J. Am. Chem. Soc.* **70** 2249–52
[16] Mudgil D, Barak S and Khatkar B S 2014 Guar gum: processing, properties and food applications - a review *J. Food Sci. Technol.* **51** 409–18
[17] McCleary B 1979 Enzymic hydrolysis, fine structure, and gelling interaction of legume-seed d-galacto-d-mannans *Carbohydr. Res.* **71** 205–30
[18] Dea I C M and Morris E R 1977 Synergistic xanthan gels *Extracellular Microbial Polysaccharides* (Washington, DC: American Chemical Society) pp 174–82
[19] Baker C W and Whistler R L 1975 Distribution of D-galactosyl groups in guaran and locust bean gum *Carbohydr. Res.* **45** 237–43
[20] Cairns P, Miles M J and Morris V J 1986 Intermolecular binding of xanthan gum and carob gum *Nature* **322** 89–90
[21] Cairns P, Miles M J, Morris V J and Brownsey G J X 1987 Ray fibre-diffraction studies of synergistic, binary polysaccharide gels *Carbohydr. Res.* **160** 411–23
[22] Tako M, Teruya T, Tamaki Y and Ohkawa K 2010 Co-gelation mechanism of xanthan and galactomannan *Colloid Polym. Sci.* **288** 1161–6
[23] Tako M 1993 Binding sites for mannose-specific interaction between xanthan and galactomannan, and glucomannan *Colloids Surf.* B **1** 125–31
[24] Grisel M, Aguni Y, Renou F and Malhiac C 2015 Impact of fine structure of galactomannans on their interactions with xanthan: two co-existing mechanisms to explain the synergy *Food Hydrocolloids* **51** 449–58
[25] Lopes L, Andrade C T, Milas M and Rinaudo M 1992 Role of conformation and acetylation of xanthan on xanthan-guar interaction *Carbohydr. Polym.* **17** 121–6
[26] Teckentrup J, Al-Hammood O, Steffens T, Bednarz H, Walhorn V, Niehaus K and Anselmetti D 2017 Comparative analysis of different xanthan samples by atomic force microscopy *J. Biotechnol.* **257** 2–8
[27] Moffat J, Morris V J, Al-Assaf S and Gunning A P 2016 Visualisation of xanthan conformation by atomic force microscopy *Carbohydr. Polym.* **148** 380–9
[28] Wehr R 2017 Korrelation der Primärstruktur von Xanthanen mit deren Verhalten in Lösung *Thesis* Johannes Gutenberg-Universität Mainz, Mainz, Germany
[29] Metzger T 2010 *Das Rheologie Handbuch: Für Anwender von Rotations-und Oszillations-Rheometern* (Hannover: Vincentz Network)
[30] Morrison N A, Clark R, Talashek T and Yuan C R 2004 New forms of xanthan gum with enhanced properties *Gums and Stabilisers for the Food Industry* vol 12 (Cambridge: Royal Society of Chemistry) pp 124–30